

COMPARISON OF BEAM-COLUMN JOINT PERFORMANCE IN A SUBASSEMBLY AND IN A FRAME

Alex V. SHEGAY*¹, Tomoyasu NISHIDA*², Hiroki KAGAWA*³ and Masaki MAEDA*⁴

ABSTRACT

The capacity of reinforced concrete (RC) beam-column joints is critical to the design and assessment of RC structures. The response characteristics that have shaped the AIJ concrete standard, as well as the understanding of damage progression have been largely based on experiments on beam-column joint subassemblies. To understand whether the beam-column joint subassembly experiments are an accurate representation of joint performance, a one-bay RC frame comprising of four beam-column joints was tested under a variable axial load.

Keywords: beam-column joints, variable axial load, reinforced concrete, RC frame

1. INTRODUCTION

Beam-column joints are an integral part of reinforced concrete (RC) frame structural systems that are designed to resist lateral loads. Capacity design principles state that as long as the expected flexural hinging capacity of the column exceeds that of the beam, and the shear capacity of the beam-column joint region exceeds maximum beam shear demand, hinging will localize in the beams such that a global sway-frame mechanism will form. In this scenario, the lateral seismic capacity of the frame can be calculated by considering beam flexural strengths alone. A culmination of database work by Fujiwara et al. [1] shown in Fig. 1 demonstrated that even when the joint shear capacity is up to 1.5 times larger than the joint shear demand, the maximum storey shear capacity (expected from a beam-yielding mechanism) may not always be attainable as damage can still concentrate in the joint region.

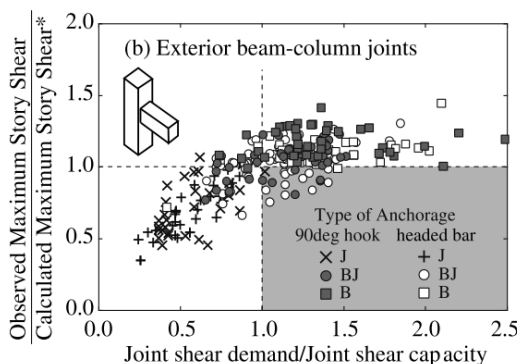


Fig. 1 Observed to calculated storey shear capacity over varying joint shear overstrength ratio.

In subassembly tests where significant joint

reinforcement yielding and concrete crushing occurs in the joint region the axial load carrying capacity through the joint can decrease. When the applied axial load can no longer be supported by the joint, the RC frame in the building becomes prone to collapse (i.e., an axial collapse mechanism). Such a failure mode is catastrophic for a building as it violates life-safety design requirements; thus, it is crucial to be able to identify joint parameters that can lead to this undesirable failure mode

A summary of failure mode for recent joint subassembly test data shown in Fig.2. The results in this figure suggest that it is possible to identify the likely failure mode of a beam-column joint by the magnitude of axial load ratio and the ratio of joint transverse reinforcement area to the beam flexural reinforcement area. In reality, joints in buildings are interconnected within frames, so demands (and consequently damage) can redistribute throughout the frame. Due to this interaction between joints, the seismic performance of individual joints (e.g., failure mode, deformation capacity) may differ compared to if the joint was tested in isolation as those in Fig. 1. Therefore, the distribution of failure mode shown in Fig.2 may not necessarily represent joint behaviour in real structures. As current design methodologies are largely based on subassembly data, it is necessary to understand whether such design and performance assumptions are still applicable in system-level tests. Therefore, the objective of this study is to identify whether the behavior of a single beam-column joint subassembly can be readily extrapolated to understand the behaviour of several joints connected in a frame system. To achieve this comparison, results of a subassembly joint test are compared to the same joint tested within an RC frame.

*1 Research, Tohoku University Graduate School of Engineering, Dr.E, JCI Member

*2 Masters Student, Tohoku University Graduate School of Engineering, JCI Student Member

*3 Bachelor Student, Tohoku University Graduate School of Engineering, JCI Member

*4 Professor, Tohoku University Graduate School of Engineering, Dr.E, JCI Member.

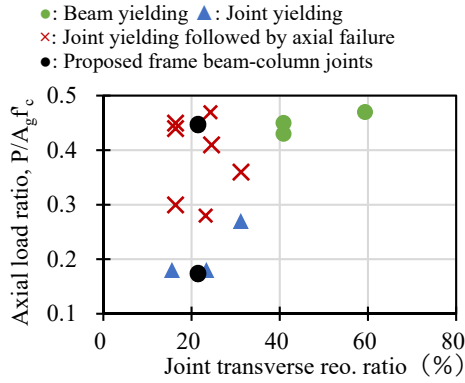


Fig. 2 Classification of recent beam-column joint subassembly tests including the specimen tested in this study.

2. TEST PROGRAM

Several recent tests of beam-column subassembly tests under variable axial load and their failure mode classifications were presented in Fig.2. In the overall study, the difference between subassembly joint performance and frame performance was considered for two axial load cases shown in Fig.2 as black dots. In this paper, the comparison for the lower axial load case (F12-20T6C2), with expected performance target of joint yielding failure, is discussed in detail. The design characteristics of F12-20T6C2 were replicating the previous subassembly beam-column test specimen T12-20T6C2 [2].

Based on this design objective, a 1/2 scale 1-bay RC frame from a 7-storey building was designed and tested to assess the performance of beam-column joints in a frame assembly. The frame comprised of four beam-column joints (1st and 2nd storey beams, and 1st, 2nd and 3rd storey columns). Inflection points were assumed at the mid-heights of the columns, so only half the 1st storey and 3rd storey columns were constructed. To simulate the zero moment condition at the column ends, pins were bolted to the steel plates that were welded to the longitudinal reinforcement of the columns. A detailed drawing of the typical beam-column joint is provided in Fig. 3 and reinforcement detail and material properties are summarized in Table 1. With exception of the concrete strength, the beam-column joints were constructed as representative as possible of the T12-20T6C2 subassembly joint previously tested [2].

Fig. 4 shows the experimental set up of the RC frame. The frame was fixed to the strongfloor through the bottom pins. Vertical and horizontal loads was applied through the top pins at the mid-height of the 3rd storey columns. Additionally, load cells capable of measuring axial and shear demands in each member were integrated into the frame at the mid-span of the 2nd storey columns and mid-span of all the beams.

2.2 Loading Method

The RC frame was subjected to cyclic, pseudo-static, in-plane loading using the set up shown in

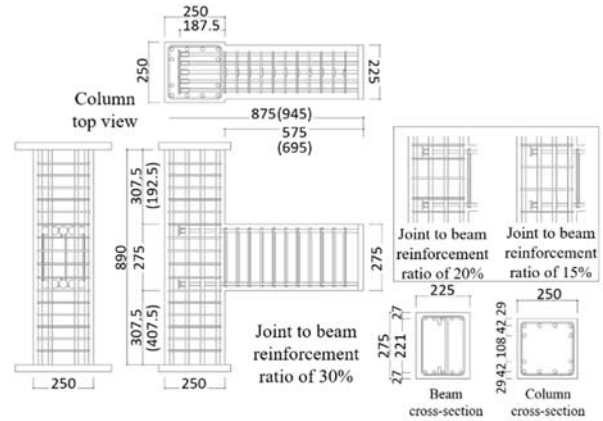


Fig. 3 Beam-column joint reinforcement design for T12-20T6C2 and F12-20T6C2. Values in brackets indicate dimensions for F12-20T6C2.

Table 1: Beam-column joint characteristics of the subassembly and frame tests.

		T12-20T6C2	F12-20T6C2
Column (250x250mm)	Long. Reo	12-D16 (SD345)	
	Transv. reo	2-D6@50 (SD295)	
	Length	1350	
Beam (225x275mm)	Long. Reo	5-D13 (SD490)	
	Transv. reo	3-D6@50 (SD295)	
	Span	1850	1900
Joint Transverse Reo		3-D6 hoops	
Joint shear capacity demand ratio		1.63	1.32
Beam-column strength ratio	Tension	1.24	1.20*
	Compression	4.77	4.05
β_j	Tension	0.89	0.88*
	Compression	1.65	1.46
f'_c , MPa		95.1	70.5
f_y (f_u), MPa	D6 (SD295)	417 (546)	438 (554)
	D13 (SD490)	535 (706)	542 (666)
	D16 (SD345)	393 (564)	390 (569)

*value corresponds to the lower joint of the frame as this is most critical in tension.

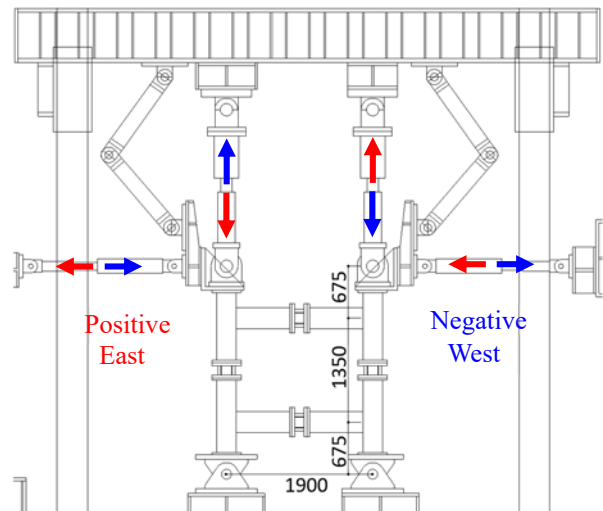


Fig. 4 Experimental set up of frame test, indicating the axial load variation in the RC frame columns as a function of lateral force.

Fig. 4. As the frame was designed to represent the exterior columns of a multi-bay frame, column axial load was varied from $0.2A_gf_c$ in compression to $0.6A_s f_y$ in tension (where A_g is the column cross sectional area, f_c is the tested concrete compressive strength, A_s is the column longitudinal reinforcement area and f_y is the tested column reinforcement yield stress), with respect to the horizontal load, as shown graphically in Fig. 5. This axial load variation is identical to that used in the beam-column subassembly T12-20T6C2 test [2]. It is noted that the axial tension and compression loads induced in the lower column of the frame would exceed the applied values shown in Fig. 5 by the magnitude of the shear force generated in the beams.

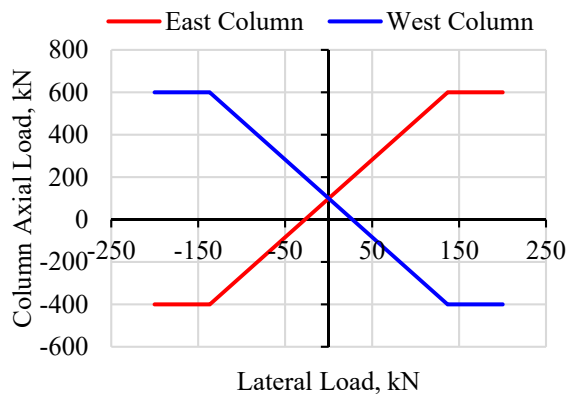


Fig. 5 Applied axial load variation in the RC frame columns as a function of lateral force.

3. RESULTS

3.1 Force-displacement response

The force-displacement characteristics of the beam-column joint subassembly test and frame test are shown in Fig. 6a and Fig. 6b, respectively. The maximum shear resistance determined from calculation (Q_{calc}) and from the experiment (Q_{exp}) are compared in Table 2. Q_{calc} was calculated assuming beam yielding governed the response of the frame, where the inflection point of the beams was assumed at the beam center and the critical beam section taken at the column face. The beam yielding moment was determined using the equivalent stress block procedures outlined in ACI-318-14 [3]. The solid red line in Fig. 6b is the summed positive and negative envelope of the subassembly test in Fig. 6a (symmetrically reflected onto the negative direction). It can be seen that the subassembly test was capable of reaching and exceeding the calculated joint capacity in the positive direction by 15%, but failed to attain the calculated capacity in the negative direction by 6%. In the negative direction, the tension force applied to the joint reduces the joint shear capacity such that it falls below the shear force required to yield the beam. Consequently, the joint region experiences yielding, which reduces the overall joint capacity. In a pure beam bending mechanism, the variable axial load will not manifest in a significant change in response in the

negative and positive directions.

Overall, there is reasonable agreement between the joint subassembly response and the frame response, thus validating the accuracy of the loading conditions used in the subassembly test. The maximum lateral strength of the frame in the negative direction is very close to the summation of the positive and negative maximum resistance of the subassembly single joint test, as can be seen in Table 2. However, contrary to the expectation of symmetry in response, in the positive direction the frame strength is higher than in the negative direction by approximately 8%. This may be attributed to initial yielding damage of the joint in tension after the first positive cycle, which reduces the global capacity of the frame in the negative cycle. This hypothesis is supported by the fact that the global positive and negative strengths of F12-20T6C2 equilibrate on the second repeated cycle. Regardless, the frame was able to achieve and exceed the β_j factor-modified shear capacity (indicated by the red dashed line in Fig. 6b), where the β_j factor is a reduction factor proposed by Shiohara and Kusuhara [4] to account for the reduction in joint strength as a result of joint yielding. The unmodified storey shear capacity (indicated by the black dashed line) was also exceeded in both loading directions.

Table 2: Calculated and observed beam-column shear capacity of the subassembly and frame tests.

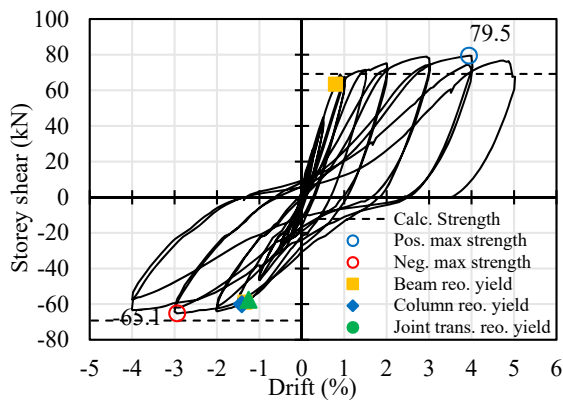
	Storey shear capacity, kN	
	T12-20T6C2	F12-20T6C2
Q_{calc}	69.2	136.8
$\beta_j Q_{calc}$	-	128.6
$+Q_{exp}$	79.5 (144.6)*	156.3
$-Q_{exp}$	65.1 (144.6)*	145.1
$+Q_{exp}/Q_{calc}$	1.15	1.14
$-Q_{exp}/Q_{calc}$	0.94	1.06

*Value in brackets is the summation of maximum positive and minimum negative shear capacity.

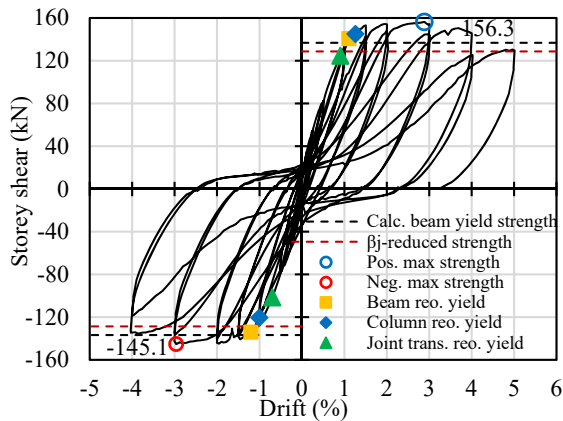
In Japanese design practice using the capacity spectrum method, maximum design drifts typically fall in the range of 1.0-2.0%. In this range of the experimental data in Fig. 6, a considerable difference in response is observed between the subassembly joint and RC frame tests as evident by the red line envelope plotted on Fig. 6b. The RC frame test rapidly reaches the unreduced calculated storey shear resistance at +1.0% drift (+129 kN) and the β_j -reduced capacity in the negative direction at -1.0% drift (-123 kN). Comparatively, while the subassembly test reaches the calculated strength at +1.0% (+69.2 kN), because the capacity in tension is low in the -1.0% drift direction (-45 kN), the equivalent 'frame' capacity is 11% below the β_j -reduced calculated value (114.2 kN).

By $\pm 1.5\%$ drift, maximum strength of F12-20T6C2 is practically achieved in both directions. This strength exceeds the calculated strength values by 10%

(+151 kN) and 2% (-140 kN) in the positive and negative directions, respectively. Comparatively at 1.5% drift, the subassembly joint test achieves +69.2 kN and -59.3 kN and in the positive and negative directions, respectively, which is an equivalent frame capacity of 128.5 kN. This experimental result is a near perfect match to the β_j -reduced calculated value in Table 2. Unlike the frame test where the shear capacity remains constant until decline at 3% drift, the subassembly joint strength continues to increase until 4% drift at which point strength degradation begins. These results suggest that joint response characteristics based on studies of subassembly beam-column joints may tend to underestimate the strength and stiffness characteristics of the beam-column joints in the 0-2% drift range. Such a conservative approach is deemed not to be detrimental to the design of frame structures.



(a) T12-20T6C2 subassembly joint



(b) F12-20T6C2 frame joint

Fig. 6 Force-displacement response of the subassembly beam-column joint and RC frame test.

3.2 Damage Characteristics

Key damage characteristics at each drift are summarized in Table 3. The drift-by-drift damage progression characteristics are generally similar between the two specimens. The exception is beam cracking observed earlier in specimen T12-20T6C2 (0.125% drift) than in specimen F12-20T6C2 (0.25% drift). It is suspected that the observed cracks were pre-existing in specimen T12-20T6C2 in the form of shrinkage cracks (as higher strength concrete was used

compared to F12-20T6C2). At the conclusion of both the subassembly and the frame tests, significant spalling damage was observed in the joint exposing longitudinal reinforcement. Warping of the longitudinal reinforcement inside the joint was perceptible due to high lateral deformation demands; however, because axial failure did not occur, localized buckling of longitudinal reinforcement or fracture of joint transverse reinforcement was not observed.

Table 3: Damage characteristics observed during testing.

Drift	Damage Observation	
	T12-20T6C2	F12-20T6C2
0.125 %	Beam cracking observed	No cracking observed
0.25%		Beam cracking
0.5%		Diagonal cracks in joint
1.0%	Yielding of beam and column longitudinal reinforcement Diagonal cracking in joint	Yielding of beam and column longitudinal reinforcement
1.5%	Increasing residual crack width No new cracks observed in joint	Increasing residual crack width Formation of new cracks
2.0%	Formation of diagonal failure plane in joint	Formation of diagonal failure plane in joint Spalling of joint region
3.0%	Spalling of joint concrete	Spalling of joint and column concrete
4.0%		Severe spalling of joint, with a gradual reduction in strength

3.3 Cracking Pattern

Typical cracking patterns of the subassembly and RC frame beam-column joint after 2.0% drift are shown in Fig. 7a and Fig. 7b, respectively.

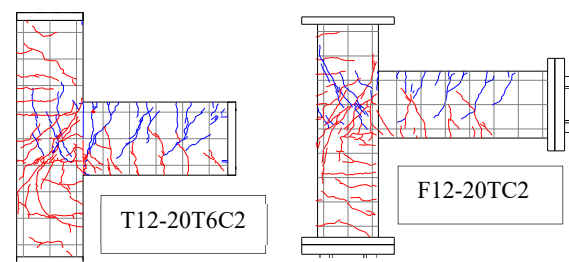


Fig. 7 Cracking patterns at 2.0% drift of (a) T12-20T6C2 subassembly joint; (b) F12-20T6C2 frame joint.

It can be visually observed that generally the crack pattern is similar between the subassembly joint test and the frame test; thus, indicating similar local stress paths in the two tests. A key difference is the positive direction (column in tension) crack pattern in the joint of the frame test (indicated in blue), which appear to align diagonally compared to the vertical crack orientation in the subassembly test. This is may be

attributed to a higher joint shear capacity ratio in the subassembly test compared to the frame test as indicated earlier in Table 1, and is the result of increased joint deformation discussed later.

3.4 Failure mode

The typical final failure mode of the joint in the frame test and in the subassembly joint is shown in Fig. 8a and Fig. 8b respectively. In both cases, as the deformation demands increased, damage began to progressively concentrate in the joint region. This was characterized by increasing crack widths, and spalling of the joint region. As the joint accumulated damage, slight strength degradation was observed on the first cycle to 4% drift for the subassembly joint test and 3% drift for the frame test. Earlier strength degradation in the frame test could be the result of additional demands in the joint from the axial force induced in the beams of the frame. After the strength degradation initiated in both experiments, damage concentrated in the joint only, experiencing considerable spalling and increased sliding characteristics along the joint shear plane. As a result of this failure mechanism, strength degradation was gradual for both experiments, as can be seen in Fig. 6. Despite the lower two joints being subjected to higher tensile and compression forces than the upper joints, damage distribution was consistent between all four joints. Even when severe damage was present at termination of the test, the deformation contribution of the upper and lower joints to the overall specimen drift was unchanged from the earlier cycles with less joint damage. After yielding of the frame, the 1st storey compression columns consistently carried approximately 90% of the total base shear while the 1st storey tension column carried the remaining 10%. Lateral resistance first dropped below 80% of the previous maximum on the second cycle to 4% for the frame test and on the first cycle to 5% in the subassembly test. It should be noted that the full axial load could still be maintained by the joints at the termination of the tests.

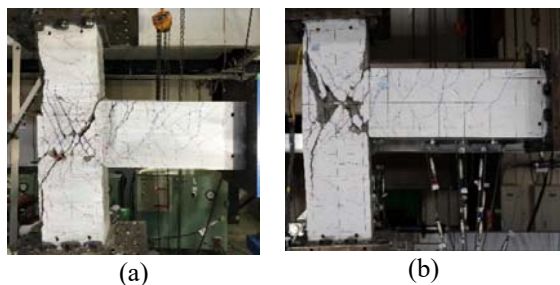


Fig. 8 State of beam-column joint at failure at 5% drift, (a) T12-20T6C2; (b) F12-20T6C2.

3.5 Stiffness characteristics

The stiffness evolution of the beam-column joint in the subassembly test and the frame test are compared in Fig. 9a and Fig. 9b for the column in compression and in tension conditions, respectively. Other than a low stiffness in the compression direction of the positive direction in Fig. 9a (attributed to a data

discrepancy), the stiffness evolution of both the subassembly test and the frame test show excellent correlation. This indicates that joint stiffness characteristics can be readily attained from subassembly tests.

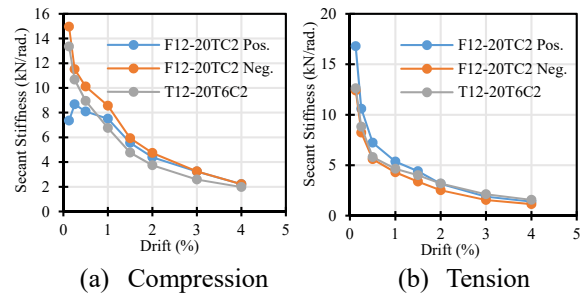


Fig. 9 Joint stiffness degradation over the duration of the beam-column joint test.

3.6 Deformation Components

The contribution of column, beam and joint deformation to the total beam-column joint drift is summarized in Fig. 10a and 10b for the subassembly joint and the frame joint (upper left joint in Fig. 4), respectively.

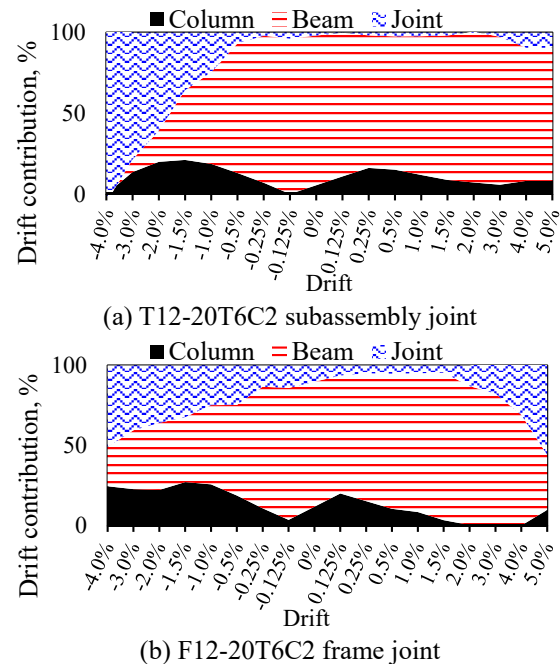


Fig. 10 Deformation component contributions to the total beam-column joint drift.

For the joint in tension case, data from the subassembly experiment shows that global drift becomes increasingly controlled by joint deformation as drift demands increase. Above 3.5% drift all of the joint drift is derived from joint deformation. Generally, the same trend is observed in the frame experiment (Fig. 10b), although the final joint deformation proportion is smaller than in the subassembly test. The principal reason for the gradual increase in joint deformation is that the joint experiences significant damage and stiffness loss under axial tension demands.

For the joint in compression case, the

subassembly joint test deformation components are approximately constant over the full drift history, and response is dominated by the bending of the beams. Comparatively, the frame joint matches the subassembly test deformation distribution only up until around 1.0% (corresponding to yielding of column reinforcement), after which joint deformation rapidly increases as can be seen in Fig. 10b. The principal reason for this joint deformation increase under compression loading (and also lower joint deformation in the tension case as mentioned above) is that unlike in the subassembly test where the location of the beam inflection point is constant, the beam inflection point in the frame test migrates towards the tension joint. This results in asymmetry in the beam bending moment distribution, with higher joint moment demands (and thus more joint deformation) in the compression load case and lower joint moment demands (and thus less joint deformation) in the tension load case, compared to the subassembly test.

3.7 Compression force induced in beams

A key response quantity that cannot be determined from a subassembly beam-column joint test is the axial force that is induced inside horizontal beams during deformation of the frame. The load cells installed throughout the frame allowed this force to be quantified. The axial load history of the upper beam in the frame is plotted in Fig. 11.

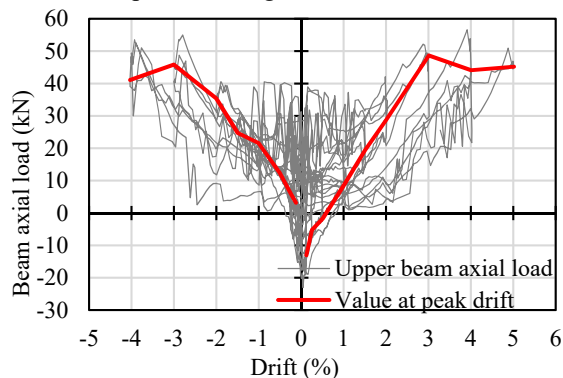


Fig. 11 Axial load in the upper beam over the course of the test.

From Fig. 11 it can be observed the axial force increase with increasing drift demands. The beam axial load accumulates as yielding of the beam longitudinal reinforcement forces the beam member to expand against the restraint provided by vertical columns. A maximum axial force of approximately 45 kN is induced at 3% drift, and remains constant until the test is terminated at 5% drift. The axial force plateaus after 3% because the deformation becomes increasingly controlled by the progressive yielding of the joint as opposed to yielding of the beam hinges. This is clearly visible in Fig. 10 where joint shear deformation starts to govern the total drift of the RC frame.

4. CONCLUSIONS

(1) Unlike the subassembly test, the RC frame test

was able to attain the full calculated storey shear capacity in both directions. The strength in the negative direction of the frame tests matched well with the positive direction of the subassembly beam-column joint, while the positive direction of the frame exceeded the subassembly joint strength by approximately 8%.

- (2) Strength and stiffness estimations of the beam-column joint using expressions developed from subassembly tests may tend to underestimate the true values expected in RC frame joint assemblies, in the 0-2% drift range.
- (3) Joint stiffness characteristics provided an excellent match between the subassembly test and the frame tests, indicating that stiffness can be reliably used from subassembly joint tests.
- (4) The joint drift in the subassembly test is governed by beam bending when the joint is in compression and joint shear deformation when the joint is in tension. Initially, the frame test shows the same tendency up until approximately 1.0% drift at which point column reinforcement yields. Following this, the moment inflection point in the beams shifts closer to the tension joint, forcing larger moment demands into the compression joint. These effects result in a rapid increase of joint deformation in the compression joints.

5. ACKNOWLEDGEMENT

The authors acknowledge the support of Mechanical Anchor Method Committee (Chair: Masaki Maeda, Secretariat: New Tech Research Group).

6. REFERENCES

- [1] Fujiwara, K., Kusuhara, F., & Shiohara, H., "Analysis on ultimate strength of reinforced concrete exterior beam-column joints by experimental database (in Japanese)," *Proceedings of the Japan Concrete Institute Conference*, vol. 33, no. 2, pp. 367–372, 2011.
- [2] Nishida, T., Suzuki, Y., & Maeda, M., "変動軸力の大きさが接合部降伏するト形柱梁接合部の破壊性状及び構造性能に与える影響に関する実験的検討," in *JCI Conference Proceedings*, 2019, vol. 41, no. 2, pp. 253–258.
- [3] American Concrete Institute (ACI), "Building Code Requirements for Structural Concrete and Commentary, ACI 318-14." ACI 318-14, Naples, FL, 2014.
- [4] Shiohara, H. & Kusuhara, F., "The next generation seismic design for reinforced concrete beam-column joints," in *Tenth U.S. National Conference on Earthquake Engineering*, 2014.